doi:10.1017/S1431927615007461 Paper No. 0667 Microsc. Microanal. 21 (Suppl 3), 2015

TEM Characterization of ion radiation damage in $Ca_{(1-x)}La_{2x/3}TiO_3$ Perovskites

Mohsen Danaie[1], Stella Pedrazzini[1], Neil P. Young[1], Paul A. J. Bagot[1], Karl R. Whittle[2] and Philip D. Edmondson[3]

[1.] University of Oxford, Department of Materials, Oxford, UK
[2.] Department of Engineering Materials, University of Sheffield, Sheffield, UK
[3.] Materials Science and Technology Division, Oak Ridge National Laboratory, Oak Ridge, USA

Perovskite phases- generic formula ABO_3, with both A and B denoting cation species- can find diverse applications both in fission and fusion nuclear energy production. Perovskites have been considered as potential matrix candidates for inert matrix fuel designs [1] and also, among other ceramics, as a more suitable encapsulation media for high-level nuclear waste disposal [1, 2]. A number of high-temperature superconducting Perovskites have also been proposed in the design of the magnetic containment of plasma in fusion energy reactors [3]. In all of the applications above, the Perovskite phase would need to withstand high doses of radiation exposure and potential incorporation of inert gases, e.g. Xe and Kr, produced during various nuclear reactions. Upon accumulation of a critical dose of radiation damage, the structure would inevitably undergo a crystalline-to-amorphous phase transition. Understanding the characteristics of this phase transformation is the key to the successful engineering application of Perovskites, as amorphisation is normally accompanied by volume change, cracking, and reduced thermodynamic stability.

The main importance of the Perovskite crystal structure lies in the tunability of this system, both with regards to introducing point defects, e.g. by having partially vacant cationic A sites, and also in the ability in changing the crystal structure by varying composition or temperature. The presence of vacancies plays an important role in the amorphisation process of irradiated Peroskites. Presence of large population of vacancies, given the high mobility of these point defects, can result in structural healing of the atomic displacements caused by the knock-on damage, as was reported in $La_xSr_{(1-3x/2)}TiO_3$ for $x \leq 0.2$ [4].

Pellets of $Ca_{(1-x)}La_{2x/3}TiO_3$ (CLTO) were synthesized via the standard solid-state ceramic routes, yielding compositions of x=0.1, 0.5, 0.7, and 0.8. Half of the pellets were irradiated with Xe^+ ions with the energy of 400 keV with 10^{15} ions/cm^2 fluence at room temperature (University of Surrey ion beam centre). Transmission electron microscopy (TEM) samples were prepared by tripod polishing followed by ion milling. A JEOL 2100 microscope, operated at 200 kV, equipped with an X-ray energy-dispersive spectrometer (XEDS), was used for microstructure characterization.

The pristine state of the CLTO phases was characterized using both XEDS and selected area diffraction (SAD). Figure 1 shows that the distribution of the constituent elements is uniform across bulk of the specimen, with compositions close to the nominal values. Electron diffraction pattern from the same area in Figure 1 can be closely indexed as the Orthorhombic Cmmm (65) crystal structure reported in [5] (Figure 2(A)). This was confirmed by examining various zone axes, one case shown in Figure 2(B). Irradiated samples showed evidence of amorphisation, with the depth of damage providing close match with the SRIM predictions. Mechanisms of crystalline-to-amorphous phase transition in CLTO will be further discussed.

References:

[1] RC Ewing, Progress in Nuclear Energy **49** (2007), p.635.
[2] WJ Weber, RC Ewing, CRA Catlow, *et al.*, Journal of Materials Research **13** (1998), p.1434.
[3] R Fuger, M Eisterer, HW Weber, IEEE Transactions on Applied Superconductivity **19** (2009), p. 1532.
[4] KL Smith, GR Lumpkin, MG Blackford, *et al.*, Journal of Applied Physics **103** (2008), 083531.
[5] Z Zhang, GR Lumpkin, CJ Howard, *et al.*, Journal of Solid State Chemistry **180** (2007), p. 1083.

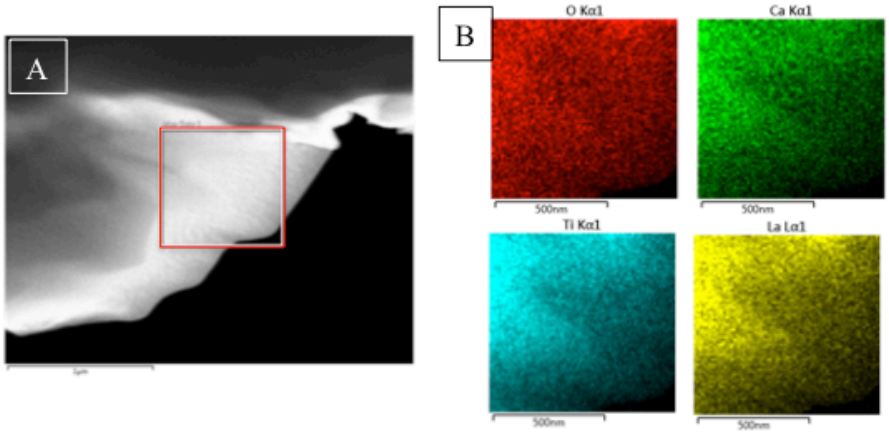

Figure 1. CLTO-X=0.7 pristine sample: (A) STEM-ADF image, (B) XEDS elemental maps of the area marked in (A).

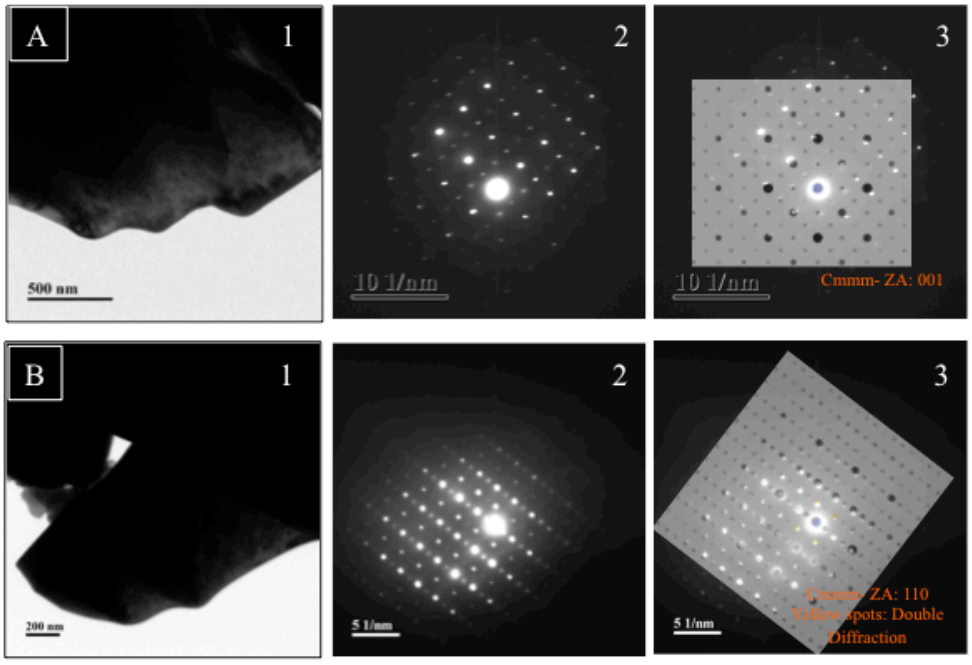

Figure 2. CLTO-X=0.7 pristine sample: (A) Same area as observed in Figure 1: (1) bright-field image, (2) SAD pattern, and (3) SAD with simulation. (B) Another area in the same sample, (1) through (3) same as panels in (A).

https://doi.org/10.1017/S1431927615007461 Published online by Cambridge University Press